Experiments and identification in micro powder injection moulding from stainless steel powder 5µm size.

C. Quinard[1], T. Barrière[1], J.C. Gelin[1]

[1]*Femto ST Institute / Applied Mechanics Department, ENSMM, 24 chemin de l'Epitaphe, 25000 Besançon*
URL: www.femto-st.fr *e-mail: jean-claude.gelin@univ-fcomte.fr*

ABSTRACT: Research tasks at ENSMM/LMA are focused on the development of mixtures of very fine powders associated to polymer binders dedicated to the powder injection micro-moulding (µPIM) in accordance with many works already carried out with different feedstock suppliers dedicated to the macro-components. Other research parts are the measurement of the shrinkage rate for cylindrical specimen in dilatometer during sintering stage and the beam bending tests during sintering process for to determine the viscosity of the sintered parts at high temperatures. It is important work to identify the constitutive law in a thermo-elasto-viscoplastic sintering model for the prediction of the shrinkage, relative density, the final residual stress and the deformation of the micro components.

Key words: Powder/binders Feedstocks, Injection Moulding, Sintering.

1 INTRODUCTION

The micro powder injection moulding (µPIM) allows the manufacturing of 3D micro-components at near netshape. This process includes four stages: the mixture of metal powders and thermoplastic binders to get feedstock, injection of powder/binder mixtures with a micro-injection moulding equipment, thermal debinding and final solid state sintering. The µPIM process can manufacture large amount of micro-components by the replication of die cavity mould [1-4].
The powders used for the mixtures are fine 316L stainless steel powders with average particle size of 5 micrometers, provided by the Osprey® Company. The binders used are from three categories: primary binders (polypropylene), secondary binder (paraffin wax) and surfactant (staric acid).
For the constitutive law identification in a thermo-elasto-viscoplastic sintering model, some dilatometer tests and beam bending tests are realized [5]. The dilatometer tests allow measuring the shrinkage rate during the sintering stage and so to determinate the sintering stress. The beam bending tests allow measuring the deflection of the components during the sintering and to determinate the uniaxial viscosity. These different parameters are used for the simulation. Numerical simulations of powder injection moulding experiments are carried out using a biphasic flow approach, in order to determine optimal mould geometries as well optimal processing conditions.

2 EXPERIMENTS

2.1 Powder characteristics and mixture stage

A 5 µm 316L stainless steel powder has been used to elaborate the feedstock. This powder has a spherical shape and is dedicated to the injection of micro-components (Table1).

Table 1. Characteristics for 316L stainless steel powders used.

Size, µm	D10, µm	D50, µm	D90, µm	Density, $g.cm^{-3}$
5 µm – 80 %vol	1.8	3.4	6.0	7.9

A formulation has been proposed for the mixtures µPIM that is composed by primary binder, secondary binder and surfactant and has a powder loading of 60% [3]. The binder is constituted by 40% polypropylene (PP), 55% paraffin wax (PW) and 5% staric acid (SA). The primary binder (PP) is used to keep the component shape after injection moulding and debinding. The secondary binder (PW) decreases the feedstock viscosity and permits the flow of the powder particles in the mould. The surfactants (SA) that improve powder wetting are very valuable. This formulation well suited for the thermal debinding is then selected. Equipment used to mix feedstock is a Z-blade mixer. The feedstock is mixed at 150°C [4-6].

2.2 *Injection stage*

The mould with the micro-cavities corresponding to two tensile and two bending test specimens is designed in the laboratory. It has been manufactured by WEDM and HSM machining. The tensile and bending specimens have been used for mechanical tests such as tensile and bending tests. Micro-components have been injected with the feedstock of powder 5µm size, the injection temperature is 190°C, and the mould temperature is 65°C. The injection pressure is 100 Mpa, the injection flow rate is 20 cm^3/s and the circumferential screw speed is 10 m/min (screw diameter is 15 mm and screw length is 600 mm). The total injected volume is about 2 cm^3.

2.3 *Debinding stage*

The debinding is used to remove the binder in the part after injection moulding. After debinding, only the primary binder (PP) and the powder remain in the component [7-9]. The thermal debinding is selected for the sake of its simplicity, safety and respect to the environment. The debinding has been realized in an oven at 220°C in argon atmosphere. The debinding temperature cycle is consisted of two stages: 2 hours heating from ambiant temperature to 130°C and 24 hours heating from 130°C to 220°C. Debinding process results in an anisotropic shrinkage. After debinding, a weight loss of 78% was observed on components.

2.4 *Sintering stage*

The sintering comes from solid state diffusion of the powder [9]. The different sintering cycles are shown at Table 2.

Table 2. Description of four different sintering cycles used for 316L stainless steel

Cycle	5°C/min	8°C/min	10°C/min	12°C/min
Ramp temp.1, °C/min	2.5	4	5	6
Set point 1, °C			600	
Dwell 1, min			30	
Ramp temp.2, °C/min	5	8	10	12
Set point 2, °C			1360	
Dwell 2, min			120	

The sintering is carried in a high temperature furnace at vacuum state. After sintering, the pure metallic components have obtained with more than 10% shrinkage. The furnace vacuum degree is 10^{-3} mbar and the alumina plate has been used for sintering support. The debinded components have been sintered with four different temperature cycles. In all cases, the maximum sintering temperature is chosen at 1360°C with 2 hours of holding time. The cooling cycle is 10°C/min cooling rate to ambient temperature. Dimension specimens have been measured after sintering, see Table 3. The average shrinkage referring to mould dimensions are between 12.33 % and 14.42 %. The shrinkage increases globally when the sintering heating rate increases, see Fig 1 and Table 3.

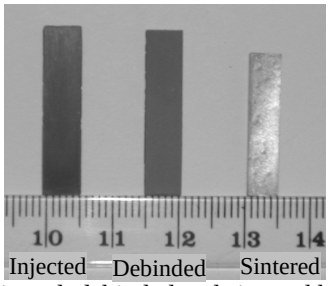

Fig 1. Injected, debinded and sintered bending test specimens realized with feedstock of powder size 5µm, sintering kinetic at 10°C/min.

Table 3. Shrinkage after sintering of components realized with feedstock of powder 5µm size, measured by vernier calliper (± 0.1 mm)

Cycle		5°C/min	8°C/min	10°C/min	12°C/min
Dimension, mm	Length	21.68	21.48	21.26	21.42
	Width	4.88	4.83	4.84	4.80
	Thickness	0.87	0.85	0.84	0.84
Shrinkage, %	Length	13.48	14.24	15.04	14.48
	Width	12.32	13.10	12.95	13.71
	Thickness	12.33	13.72	14.43	15.14
	Average	12.33	13.41	13.74	14.42

3 MODELLING AND IDENTIFICATION

3.1 *Modelling of sintering process*

The sintering for solid state diffusion is modelling with viscoplastic constitutive law [5], determinate for the inverse expression of the Hooke's law, expressed in Equation (1):

$$\dot{\varepsilon}^{vp} = \frac{\sigma'}{2G} + \frac{\sigma_m - \sigma_s}{3K} I \qquad (1)$$

where σ' = deviatoric stress tensor, G = shear viscosity modulus, σ_m= hydrostatic stress, σ_s = sintering stress. K = bulk viscosity modulus and I = second order identity tensor. The shear and bulk viscosity modulus is expressed with following Equations (2) and (3):

$$G = \frac{\eta_p}{2(1+\nu_p)} \quad ; \quad K = \frac{\eta_p}{3(1-2\nu_p)} \qquad (2)\ (3)$$

where η_p = is uniaxial viscosity and υ_p = Poisson's ratio of porous material. The Poisson's ratio of the sintering material can be expresses by the following Equation (4):

$$\nu_p \approx \frac{1}{2}\sqrt{\frac{\rho}{3-2\rho}} \quad (4)$$

where ρ = relative density, increases from 0.6 and 1. The uniaxial viscosity can be expressed as (5):

$$\eta_p = \frac{kTG^3\rho^2}{47.5V_a\delta_b D_{b0}\exp(-Q_b/RT)} \quad (5)$$

where k = Bolzmann's constant, T = absolute temperature, G = grain size, ρ = relative density, V_a = atomic volume, δb = thickness of grain boundary, D_{b0} = grain boundary diffusion frequency, Q_d = activation energy for grain boundary diffusion. The grain growth behaviour of 316L stainless steel powders during sintering can be expressed from the following Equation (6):

$$\frac{dG}{dt} = \frac{A\exp(-Q_G/RT)}{G} \quad (6)$$

where Q_G = grain growth activation energy. When the temperature is less than 1200°C, Q_G = 315.8 kJ/mol, otherwise Q_G = 50 kJ/mol, A = material constant. The sintering stress is determinate in a function of relative density and particles size, expressed in Equation (7):

$$\sigma_s = \frac{C\rho^2}{r} \quad (7)$$

where r = radius of the powder particles and C = constant to be determined from the dilatometer sintering experiments.

3.2 Sintering identification by dilatometer test

Dilatometer sintering tests have been realized with feedstock of powder 5µm size. The objective is to determinate the sintering stress [10]. After debinding, the cylinder specimens (5 mm diameter and 10 mm length) have been pre-sintering: 2.6°C/min heating to 800°C, holding 30 min. The dilatometer sintering cycles have been performed with 5, 8, 10 and 12°C/min heating to 1360°C, holding 120 min, in vacuum (Fig 2).

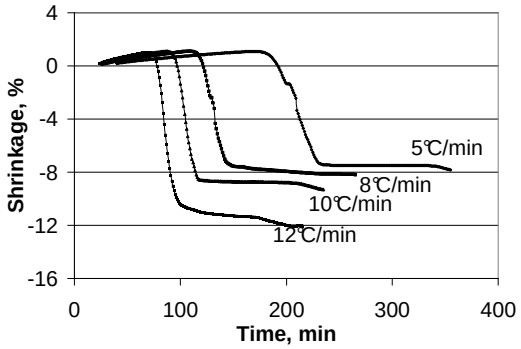

Fig 2. Shrinkage vs. time obtained at 5, 8, 10 and 12°C/min ramp temperature.

Shrinkages and shrinkage rates have been measured for the different kinetics during the sintering stage in dilatometer. The final densities of cylinders after sintering are calculated with Equation (8):

$$d_f = \frac{\Phi}{(1-\delta)^3} \quad (8)$$

where Φ = critical solid volume fraction and δ = shrinkage after dilatometer sintering. The results of shrinkages and densities are given in Table 4. The shrinkage and the densities increase according to the sintering kinetic. The shrinkages measured in dilatometer tests are lower than the shrinkages measured in PIM experiments (Table 3). This difference results from the pre-sintering at 800°C for dilatometer test where the components have low shrinkage.

Table 4. Properties feedstock of powders 5µm size after sintering at 1360°C

Ramp temperature.2	Shrinkage, %	Final density, %
5°C/min	7.83	0.89
8°C/min	8.21	0.92
10°C/min	9.31	0.93
12°C/min	12.04	0.96

3.3 Sintering identification by bending test

Beam bending tests have realized with bending specimens, after debinding, for determinate the uniaxial viscosity [10]. This test is based on the measured of deflection at the center position of the specimens (Fig 3). The uniaxial viscosity can be expressed as (9):

$$\eta_p = \frac{1}{\dot{\delta}}\left(\frac{5\rho_a g L_s^3}{32h^2} + \frac{PL_s^3}{4bh^3}\right) \text{ where } \dot{\delta} = \Delta\delta\frac{k_n}{\Delta t} \quad (9)$$

where $\dot{\delta}$ = deflection rate, $\Delta\delta$ = change in deflection, Δt = change in temperature, k_n = heating rate, ρ_a = apparent density, g = gravity acceleration, P = external load (1,75g), b and h = width and thickness of specimen, L_s = span distance of the beam (18 mm).

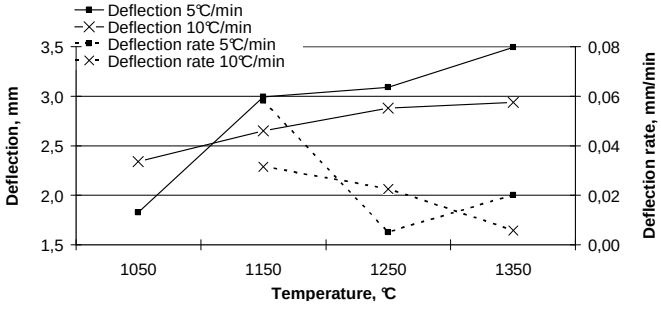

Fig 3. Deflection and deflection rate vs. time obtained at 5°C/min and 10°C/ ramp temperature.

3.4 Identification of uniaxial viscosity and sintering stress

The identification by inverse method, using the trial and error method, from equations (5) and (9), allows to determinate the uniaxial viscosity of specimen during the sintering stage (Fig 4).

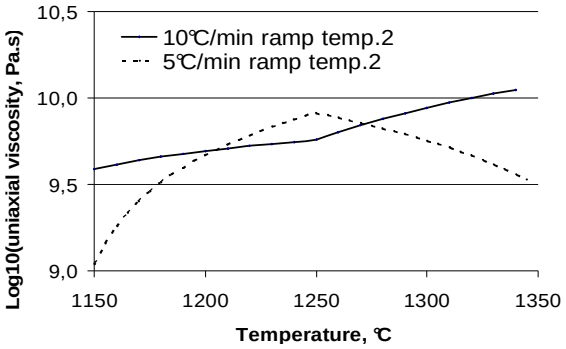

Fig 4. Uniaxial viscosity vs. temperature obtained at 5°C/min and 10°C/min ramp temperature during sintering.

By coupling the uniaxial viscosity and dilatometer sintering tests, the constant C has been identified (Table 5):

Table 5. Identified material parameter C for sintering stress for 316L stainless steel powder 5µm size.

Cycles		C (N.m^{-1})
5°C/min	heating	2.325
10°C/min	heating	21.825

These values have been in accordance with [11] obtained for 316L stainless steel powder 16µm size.

4 CONCLUSIONS

The paper demonstrates the possibility to get metallic micro-parts from µPIM process. It has been shown that the fine metallic powders can be mixed with different polymers to get feedstocks, well adapted to micro-injection. The micro-components after injection exhibit very little shrinkage and debinding and solid state sintering process are then possible. The results obtained confirm that the resulting components after debinding and sintering exhibit shrinkage in range from 12 to 15%, in a homogeneous way. More, the identification for determinate the uniaxial viscosity and the sintering stress of 5µm stainless steel powder will permit to simulate the shrinkage from the viscoplastic constitutive law for the modelling of the sintering and will permit to compare with experiments results and to determine the size of mould die cavity.

REFERENCES

1. T. Barriere, J.C. Gelin and B. Liu, Experimental and numerical investigations on the properties and quality of parts produced by MIM, Powder Metallurgy, Ed. by Maney Publishing 44, 3, 2001, pp. 228-234.
2. B. Williams, Feedstock aids microPIM parts production: Tiny cogs test the imagination of powder professionals as small parts demand ever-finer materials, Metal Powder Report, Volume 58, Issue 10, October 2003, pp. 27-28.
3. R.M. German and A. Bose, Injection Molding of Metals and Ceramics, Princeton, New Jersey, USA, 1997, pp. 1-100.
4. C. Quinard, T. Barrière and J.C. Gelin, Development of Metal/Polymer Mixtures for Micro powder Injection Moulding, 10th ESAFORM Conference on material Forming, 2007.
5. J. Song, J.C. Gelin, T. Barriere and B. Liu, Experiments and numerical modelling of solid state sintering for 316L stainless steel components, J. of Materials Processing and Technology 177, 2006, pp 352-355
6. L. Liu, N.H. Loh, B.Y. Tay, S.B. Tor, Y. Murakoshi and R. Maeda, Mixing and characterisation of 316L stainless steel feedstock for micro powder injection molding, Materials Characterization 54, 2005, pp 230-238.
7. R.M. German and A. Bose, Wick debinding distortion of injection molded powder compacts, Int. J. Powder Metallurgy 26, 1990, pp 217-230.
8. D.F. Haeney, T.J. Mueller and P.A. Davies, Mechanical properties of metal injection moulding 316L stainless steel using both prealloy and master alloy techniques, Int. J. Powder Metallurgy 47, 2004.
9. J.C. Gelin, T. Barriere, J. Song, Processing defects and resulting mechanical properties after metal injection molding, J. Eng. Materials Technology, Trans. ASME, in print, 2008, pp.1-16.
10. G. Ayad, T. Barriere, J.C. Gelin, J. Song, B. Liu, Sequential steps of optimization for consequent processing stages of powder injection molding, European Journal of Computational Mechanics, in print, 2008, pp.1-12.
11. J. Song, T. Barriere, B. Liu, J.C. Gelin, M. Gerard, Experimental and numerical analysis on the sintering behaviours of injection moulded components in 316L stainless steel powder, Powder Metallurgy, in review, February 2008, pp.1-14.